Journal of the Iranian Chemical Society (2022) 19:2383–2394
https://doi.org/10.1007/s13738-021-02457-9

ORIGINAL PAPER

A simple and straightforward combination of surfactant-assisted magnetic dispersive micro-solid-phase extraction and hydride generation procedure to determine arsenic (III) species in environmental, biological, and fruit juice samples

Fateme Fallah Tafti[1] · **Mahboobeh Masrournia**[1]

Received: 27 May 2021 / Accepted: 11 November 2021 / Published online: 31 January 2022

Abstract
Arsenic is a toxic element with various applications. Due to the high toxicity of arsenic and its species, the determination of arsenic species in real samples is significant to control their effects on the environment and human health. A surfactant-assisted dispersive micro-solid-phase extraction was utilized as a simple and efficient sample preparation method to extract and preconcentrate arsenic (III) species in environmental, biological, and fruit samples. The microextraction method was simply combined with a chemical hydride generation strategy to determine arsenic (III) species with the graphite furnace atomic absorption spectrophotometric method. A green and magnetic sorbent was synthesized based on coating the prepared magnetic Fe_3O_4 nanoparticles with chitosan using a simple and straightforward chemical procedure. Usage of surfactant as a dispersion agent in the microextraction procedure enhanced the sorbent dispersion efficiency and reduced the ultrasonic time for the sorbent dispersion. Three surfactants such as sodium dodecyl sulfate, hexadecyltrimethylammonium bromide, and triton X100 were selected as representative of anionic, cationic, and neutral surfactants, respectively, and their effects were investigated in the As(III) extraction; as a result, hexadecyltrimethylammonium bromide was chosen as the best dispersion agent. Other factors that affected the microextraction method were optimized by an experimental design strategy. Under the optimum condition, a linear range was acquired in the range of 0.009–10.0 μg mL^{-1} with a determination coefficient of 0.9903. Limit of detection, limit of quantitation, and enrichment factor for the As(III) determination with the proposed method were 0.003 μg L^{-1}, 0.009 μg L^{-1}, and 21.4, respectively. The relative standard deviation ($n=5$) for the As(III) determination with a concentration of 0.1 μg L^{-1} was equal to 3.27%. The applicability of the method for the As(III) determination was investigated by analyzing water, urine, and fruit juice samples with a relative recovery and RSD in the ranges of 94.0–97.4% and 3.17–4.54%.

Keywords Dispersive micro-solid-phase extraction · Hydride generation · Arsenic species · Fe_3O_4@chitosan · Fruit juice sample · Urine sample

Introduction

Nowadays, heavy metals have increased environmental pollution and enter into the food chains due to the rapid growth of industrial processes that lead to the risk of exposure of humans and animals to heavy metals. These elements have adverse effects on human and animal health; as a result, their measurement in various real samples such as water and biological samples with high accuracy and precision have been regarded [1, 2]. Among them, arsenic is one of the most toxic elements, increasing the risk of cancer and cardiovascular diseases [3–5]. However, most of the proposed methods with the spectroscopy technique for determining the total As content are in real samples. Therefore, the development of a new approach to measuring the As species with these techniques is very important. Also, the low concentration of As species in real samples, the high matrix effects of the real samples, and the conversion of the sample to a suitable form for presentation to the detection

✉ Mahboobeh Masrournia
mah.masrour@gmail.com

[1] Department of Chemistry, Mashhad Branch, Islamic Azad University, Mashhad, Iran

system necessitate the use of sample preparation methods [6–10]. Microextraction procedure as a sample preparation method has been developed and widely utilized for various real samples with low (or free) organic solvent consumption [11, 12]. The method can reduce the matrix effect of real samples and increase the analyte concentration simultaneously. Besides, a low amount of real samples is introduced in the microextraction procedure [13].

Dispersive micro-solid-phase extraction (DμSPE) is a widely used microextraction method in which a suitable sorbent is dispersed in the sample solution for analyte adsorption [14, 15]. In this method, the sorbent plays a critical role in an analyte extraction by creating appropriate and selective interactions with the analyte [16, 17]. Obviously, a selective interaction of sorbent with a particular metal species can lead to extract a metal species from a real sample [18, 19]. Therefore, the crucial parameter in the DμSPE procedure is the preparation of sorbent or its functionalization with proper functional groups. Usage of a magnetic core coated with a green sorbent leads to preparing a green and magnetic sorbent to simply separate sorbent under a magnetic field. Another critical parameter in the procedure is the sorbent dispersion in real samples. Vortex mixer and ultrasonic bath have been applied for the sorbent dispersion with high efficiency [20, 21]. However, the ultrasonic bath ability is greater than the vortex mixer to disperse the sorbent due to the high energy released in the sample solution using the ultrasonic bath [22]. An essential problem with the ultrasonic bath is the degradation of the sorbent or analyte in the sample solution due to the high energy released due to the formation of micro-reactors with a high temperature in the sample solution [23–25]. A suitable development to reduce the ultrasonic time of the sample solution involves the use of a suitable solvent, ionic liquid, or surfactant as a dispersion agent to assist the sorbent dispersion in the sample solution. Also, the sorbent dispersion into a suitable solvent before injecting into the sample solution is another procedure that reduces both sorbent dispersion time and sorbent contact time (extraction time) with the analyte [16, 26]. This method reduces the matrix effects of the real sample by reducing the extraction time. In other words, interfering species with a slower mass transfer than analyte will not have enough time to extract to the sorbent surface as the extraction time decreases.

Hydride generation (HG) is one of the common methods for measuring arsenic, especially for the determination of its species at low concentrations. Providing a hydride-based sample to the device improves the sensitivity and detection limit compared to the direct presentation of the sample, significantly [27]. The HG method is coupled with many methods to improve sensitivity and detection limit of As determination. The combination of HG-AAS and HG-AFS methods with different sample preparation methods such as liquid–liquid extraction [28], ionic exchange chromatography s[29, 30], and high-performance liquid chromatography [31, 32] allows the measurement of the As species with high sensitivity.

The experimental design as a suitable procedure has been widely utilized to optimize effective factors on the microextraction method due to reducing the number of experiments, material consumption, saving time, and money. Also, the procedure can be used to evaluate the interaction between factors. This method is beneficial for optimizing factors when the number of these factors is large [33]. In this case, this method is performed in two steps. At the screening stage, factors with a significant effect on the extraction process are determined. In the optimization stage, the significant factors are optimized, and the effects of these factors and their interactions on the analyte measurement are evaluated [34, 35].

In the present study, surfactant-assisted dispersive micro-solid-phase extraction as a simple and efficient sample preparation procedure was developed to extract As(III) ions from water, biological, and fruit juice samples. A green and suitable sorbent based on coating magnetic Fe_3O_4 nanoparticle as a magnetic sorbent core with chitosan prepared using a simple chemical procedure. After the As(III) extraction, a hydride generation strategy combined with the electrothermal atomic absorption spectrometric method was utilized as a sensitive detection system for the As(III) determination. The use of the microextraction method using a green adsorbent is under the principles of green chemistry. Besides, a surfactant was utilized to reduce the ultrasonic time and increase the dispersion efficiency of the sorbent in the sample solution, leading to an increase in the analyte extraction efficiency. The combination of three techniques was performed simply and without the need for sophisticated devices. The experimental design was employed to optimize ten factors that may affect the As(III) determination. The method was successfully applied to analyze several real samples for the As(III) determination without any initial preparation.

Experimental

Instruments

A Hitachi Z-2000 (Hitachi, Japan) flame atomic absorption spectrometer was equipped with a Zeeman background correction and a heated graphite tube atomizer. An arsenic hollow cathode lamp (Hitachi, Japan) at a wavelength of 197.0 nm as a radiation source, operated at 8 mA with a monochromator slit width of 1.2 nm, and a pyrolytically coated graphite tube were utilized to determine As(III) ion. The FTIR spectrophotometer (Bruker tensor model) and the

scanning electron microscopy (SEM, VP1450 model, LEO, Germany), and the transmission electron microscopy (TEM, 912 AB model, LEO, Germany) were applied for identifying the structure and morphology of the magnetic Fe_3O_4/Chitosan mesopores. A VASCO NP size analyzer (Cordouan technology, France) was utilized to investigate the sorbent particle size. A pH meter model 780 of Metrohm (Swiss) was used for adjusting the pH of the sample solution.

Materials

Chitosan was obtained from Nano Radan Co. (Gilan, Iran). Other material and reagents such as arsenic trioxide, sodium borohydride, sodium dodecyl sulfate (SDS), hexadecyltrimethylammonium bromide (CTAB), triton X100, iron (II) sulfate heptahydrate, trisodium citrate, sodium hydroxide, nitric acid, sulfuric acid, hydrochloric acid, formic acid, acetic acid, sodium acetate, lanthanum nitrate, and iridium nitrate were purchased from Merck (Darmstadt, Germany). The stock standard solution of As(III) ion (1000 mg L^{-1}, 100.0 mL) was prepared by dissolving 0.132 g of arsenic trioxide in 25.0 mL of sodium hydroxide solution (20% w/v), neutralized with sulfuric acid (20% v/v) in the presence of two drops of phenolphthalein, and diluted to 100.0 mL with distilled water. The obtained solution was diluted to 1.0 L using a sulfuric acid solution (1.0% v/v). The working standard solutions of As(III) ion were daily prepared by diluting the appropriated volume of the stock solution in a suitable volumetric balloon with distilled water.

Synthesis of Fe_3O_4 nanoparticles

Here, magnetic Fe_3O_4 nanoparticles were prepared by the co-precipitation method based on the previous lecture [36]. For this purpose, 1.47 g of trisodium citrate, 0.80 g of sodium hydroxide, and 17.0 g of sodium nitrate were poured into 90.0 mL of deionized water and stirred for 2 min, followed by heating up to 100 °C to prepare a clear solution. Afterward, 10.0 mL of an aqueous solution of $FeSO_4.7H_2O$ with a concentration of 1.0 mol L^{-1} was added to the resulting solution. The black precipitate of magnetic Fe_3O_4 nanoparticles was formed into the solution. The resulting mixture was cooled to room temperature, and the magnetic Fe_3O_4 nanoparticles were separated from the mixture by a magnet. The magnetic Fe_3O_4 nanoparticles were finally washed three times with distilled water and dried at 40 °C for 10 h.

Synthesis of Fe_3O_4-chitosan mesopores

The magnetic Fe_3O_4-chitosan mesopores were synthesized using the previous method [37]. Firstly, a solution of chitosan (5.0% W/V, 100.0 mL) was prepared from dissolving 50 mg of chitosan in acetate buffer (0.05 M, pH 4.2) using an ultrasonic bath for 30 min at room temperature. Afterward, 0.1 g of Fe_3O_4 nanoparticles were added to 10.0 mL of chitosan solution and dispersed by stirring at room temperature for 30 min and a homogenous and high viscosity mixture of chitosan along with magnetic Fe_3O_4 nanoparticles was prepared. An aqueous solution of sodium hydroxide (1.0 mol L^{-1}) was added dropwise to the mixture while the mixture was stirred at 300 rpm for 15 min. The resulting precipitate was disparted from the supernatant solution using a magnet and washed three times with an acetate buffer (pH 4). Then, 10.0 mL of deionized water and 2.0 mL of glutaraldehyde were added to the resulting precipitate to establish crosslinks between magnetic Fe_3O_4 nanoparticles and chitosan. Eventually, the mixture was mixed for 12 h by vortex mixer, and the magnetic Fe_3O_4—chitosan mesopores were gathered using a magnet. The resulting product was finally washed several times with distilled water and dried in an oven at 45 °C for 8 h.

Microextraction process

The sorbent (30 mg) and CTAB (20 mg) were poured into 1.0 mL of distilled water, followed by sonicating for 3 min to form a perfectly uniform suspension. 20.0 mL of sample solution was transferred to a suitable vial, and its pH was adjusted to 8.1 using sodium hydroxide or hydrochloric acid (0.1 mol L^{-1}). The prepared sorbent suspension was injected into the sample solution with pH 8.1 and sonicated for 5 min at room temperature. The sorbent was separated from the sample solution under a magnetic field in the presence of a neodymium magnet, and the sample solution was discarded. Then, 148 µL of nitric acid (0.5 mol L^{-1}) as a desorption solution was added to the sorbent. The mixture was sonicated for 8 min to desorb the As(III) ions from the sorbent surface. The sorbent was separated from the nitric acid phase using a neodymium magnet. The nitric acid phase was transported to three-neck flat bottom flask. A $NaBH_4$ solution (1.0%, 0.5 mL) was added to the nitric acid phase while Ar gas was entered into the flask with a rate of 1.5 mL min^{-1} for 30 s, and the produced arsine gas along with the Ar gas was transferred into the graphite furnace for analysis. The graphite furnace program for the As(III) determination was performed based on a previous lecture with a slight modification and presented in Electronic Supplementary Material (ESM Table S1)[38]. The graphite furnace surface was modified by injecting 10 µL of a solution containing lanthanum nitrate and iridium nitrate with a concentration of 1000 mg L^{-1} followed by heating for 30 s to 120 °C with a rate of 5 °C s^{-1} and 30 s to 1100 °C with a rate of 50 °C s^{-1}.

Result and discussion

Characterization of synthetic nanocomposite

IR spectrum of synthetic magnetic Fe_3O_4-chitosan mesopores is shown in Fig. 1. The bond at 3417.51 cm^{-1} can be related to the stretching vibrations of OH and the NH_2 group, which is board due to the formation of hydrogen bonds. The absorption peak at 1601.11 cm^{-1} corresponds to the vibrations of the N–H bond in chitosan. The absorption peak at 1423.45 and 1383.57 cm^{-1} is related to the stretching vibrations of the C-N bond and the deformation vibrations of N–H in the chitosan structure, respectively. The vibration peak at 1086.54 cm^{-1} refers to the stretching vibration of CO in the C–OH functional group. Also, the absorption bond in 598.18 cm^{-1} refers to the stretching vibrations of the Fe–O bond in the Fe_3O_4 nanoparticles, confirming the successful synthesis of the magnetic Fe_3O_4-chitosan mesopores.

Also, TEM and SEM images of magnetic Fe_3O_4/ chitosan are shown in Fig. 2. In TEM images (a and b) can be seen the spherical particles with a nearly homogeneous and uniform structure. Also, an aggregation of nanoparticles was displayed due to the magnetic properties of the sorbent that can lead to a reduction in the ability of the sorbent to extract the analyte. Therefore, the dispersion of the sorbent with high efficiency is necessary to obtain the proper extraction efficiency of As(III). The average size of sorbent particles was estimated at about 20 nm by TEM. In the SEM images (c and d), the formation of the chitosan layer around the magnetic Fe_3O_4 core is viewed, indicating that the sorbent includes double layers with a magnetic Fe_3O_4 core and an outer layer of chitosan.

The DLS analysis of magnetic Fe_3O_4/ chitosan without CTAB or in the presence of CTAB was investigated. The mean sizes of the magnetic particles were 14.569 and 13.598 nm without and with CTAB, respectively. The BET surface areas of the magnetic Fe_3O_4/ chitosan particles were 135.28 and 152.73 m^2g^{-1} without and with CTAB, respectively. The mean pore diameters of 21.734 and 22.409 nm were obtained for the magnetic Fe3O4/ chitosan particles without and with CTAB.

Optimization strategy of microextraction procedure

Various factors can be effective in the extraction efficiency of As (III) by the proposed method, such as pH, sample solution volume, type of acid as desorption solvent, volume and concentration of nitric acid, sorbent amount, type and volume of dispersion solvent, extraction time, dispersion time, desorption time, and salt amount. Therefore, it is necessary to consider and optimize these indented variables to obtain the highest As (III) extraction efficiency. Two factors, including the type of desorption solution and surfactant, were optimized with one factor at a time procedure (OFAT). Due to the large number of factors evaluated in the As(III) ion measurement, the optimization strategy consisted of two steps. In the first step, a Plackett–Burman design (PBD) was used to screen and determine the significant factors influencing the As(III) ion extraction process. In the second step, a central composite design (CCD) was created to optimize the effective factors of the screening step. To optimize each factor, the experiment was performed three times under the same conditions.

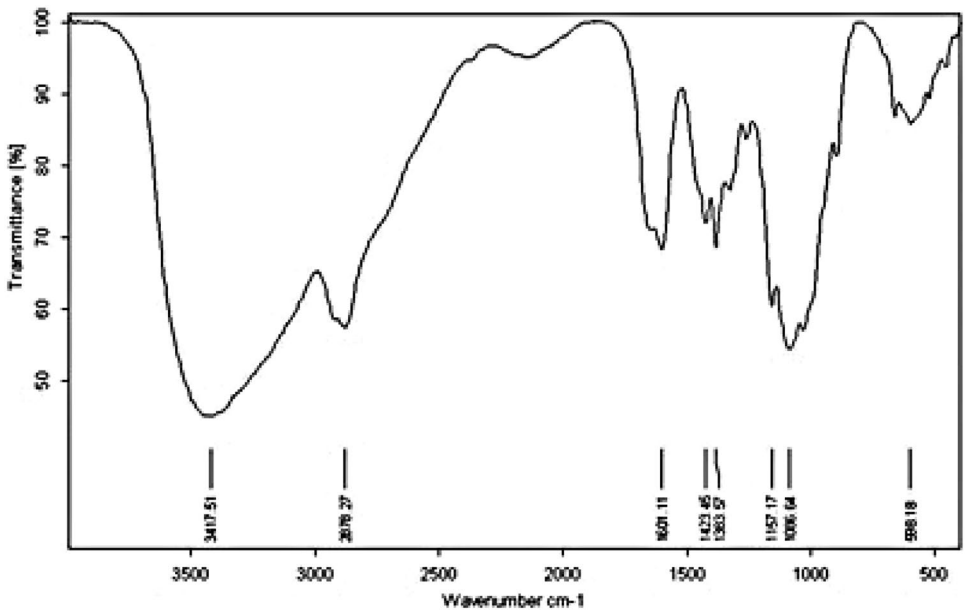

Fig. 1 FTIR spectrum of the magnetic Fe_3O_4/chitosan mesopores

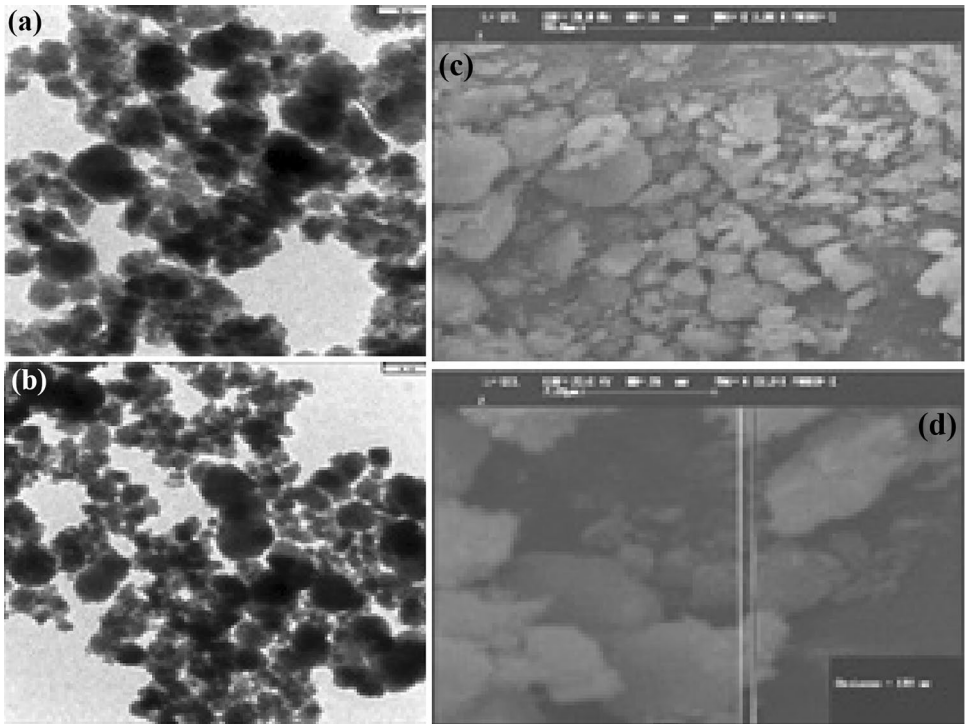

Fig. 2 TEM images (**a** and **b**) and SEM images (**c** and **d**) of the magnetic Fe_3O_4/chitosan mesopores

Type of acid solution

In the DμSPE procedure, the analyte adsorbed on the sorbent must be desorbed into a desorption solvent from the sorbent surface to determine the analyte by a detection system. In the study, several organic and inorganic acid solutions were selected as the desorption solution and their effects on the analyte desorption were evaluated (ESM Fig. S1). The results indicated that nitric acid solution has the highest extraction efficiency toward As(III) ion and was selected as a desorption solution for further study. Also, aqueous solutions of inorganic acids have higher extraction efficiencies for the As(III) ion desorption than organic solvents and organic acid solutions.

Type of surfactant

Surfactant was applied as a dispersion solvent to reduce the ultrasonication time and increase the sorbent dispersion efficiency into the sample solution. A decrease in the ultrasonic time of the sample solution leads to a reduction in the possibility of sorbent degradation in the sample solution. Also, the extraction efficiency of the analyte was increased by reducing the sorbent size into the sample solution and increasing the sorbent surface area relative to its volume. Therefore, three surfactants, such as sodium dodecyl sulfate (SDS), hexadecyltrimethylammonium bromide (CTAB), and triton X100, were selected as representative of anionic, cationic, and neutral surfactants, respectively, and their effects were investigated in the As(III) extraction (Fig. 3). The volume of SDS and triton X100 was 20 μL, and the CTAB amount was 20 mg in the study. The results showed that CTAB has the highest extraction efficiency for the As(III) determination, and SDS has the lowest extraction efficiency. At pH 4.0, this may be because SDS has a negative charge on the surface that can interact with As(III) through an electrostatic attraction. The interaction between As(III) and SDS prevents the extraction of the species formed on the sorbent surface. In contrast, the CTAB has a positive charge and does not interact with the analyte due to electrostatic repulsion between the positive charge of As (III) ion and the positive charge of CTAB. In other words, CTAB does not directly affect the analyte interaction with the sorbent surface through forming hemimicelles on the sorbent surface and only increases the analyte extraction efficiency by increasing the sorbent dispersion in the sample solution. Therefore, CTAB acts as a dispersion agent for the sorbent dispersion in the sample solution. Also, the analyte extraction efficiency without surfactant showed that using a suitable surfactant can lead to an increase in the analyte extraction efficiency by increasing the sorbent dispersion efficiency. DLS analysis indicated that the particle size of the sorbent was reduced in the presence of CTAB due to better dispersion of the sorbent in the sample solution ("Characterization of synthetic nanocomposite" Section). Also, an increase in the surface area of the sorbent with CTAB leads to an increase in the analyte extraction efficiency ("Characterization of synthetic nanocomposite" section). However, CTAB can reduce the surface tension of

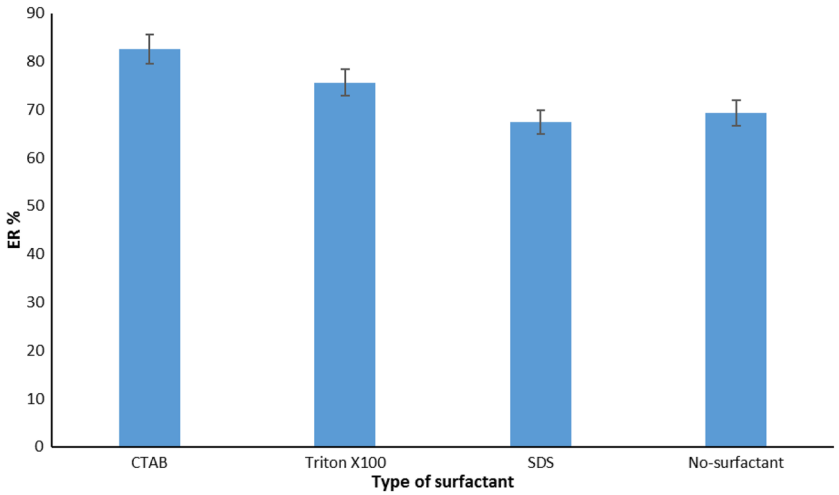

Fig. 3 The effects of surfactant type on the As (III) extraction. Condition: As(III) concentration; 30.0 ng L^{-1}, sample volume; 30 mL,, dispersion time; 5 min, extraction time; 5 min, dispersion time; 10 min, pH 4.0, desorption solution; nitric acid (0.5 Mol L^{-1}, 0.3 mL)

the sample solution to increase the sorbent dispersion efficiency. Therefore, CTAB was chosen as a suitable surfactant for further investigation.

Plackett–Burman design

In this work, ten factors were selected for the screening step. These factors and their selected level are presented in ESM Table S2. To evaluate these factors, a Plackett–Burman design (PBD) was generated with a random order of twelve experimental runs. The experimental runs of PBD and their obtained responses are shown in Table 1. Analysis of variance (ANOVA) was utilized at a 95% of confidence limit for the evaluation of factors and the determination of their significant effect on the As(III) determination[39]. The obtained results are indicated in a Pareto chart (Fig. 4). According to Fig. 4, three factors, including the pH of the sample solution (A), sorbent amount (B), and desorption solvent volume (J), have a significant effect on the As(III) determination because the bar length of these factors on the Pareto chart is passed from the reference line (vertical and dotted line) at a 95% of confidence limit ($\alpha = 0.05$). Also, the sorbent amount has the highest effect on the As(III) determination because of the largest bar length on the Pareto chart. The next important factor is the pH of the sample solution, indicating that the interaction of the sorbent with the analyte is affected by the pH of the sample solution. The desorption solvent volume is another factor with a significant effect on the As (III) measurement, which shows that the extraction efficiency of the As (III) ions increases with decreasing the desorption solvent volume. Other factors such as sample solution volume, concentration of nitric acid, amount of dispersion agent (surfactant), extraction time, dispersion time, desorption time, and salt amount have a significant effect on the As(III) determination and constant at 20 mL, 0.5 mol L^{-1}, 20 mg, 5 min, 3 min, 8 min, and 0.0% for the optimization step, respectively.

Table 1 The Plackett–Burman design matrix, along with the obtained responses for the As (III) determination

Standard order	Run order	A	B	C	D	E	F	G	H	J	K	Response%
1	1	1	−1	1	−1	−1	−1	1	1	1	−1	40.93
9	2	−1	−1	−1	1	1	1	−1	1	1	−1	48.99
3	3	−1	1	1	−1	1	−1	−1	−1	1	1	46.88
4	4	1	−1	1	1	−1	1	−1	−1	−1	1	67.23
12	5	−1	−1	−1	−1	−1	−1	−1	−1	−1	−1	38.37
5	6	1	1	−1	1	1	−1	1	−1	−1	−1	89.38
2	7	1	1	−1	1	−1	−1	−1	1	1	1	80.61
8	8	−1	−1	1	1	1	−1	1	1	−1	1	47.34
11	9	−1	1	−1	−1	−1	1	1	1	−1	1	69.15
10	10	1	−1	−1	−1	1	1	1	−1	1	1	57.91
7	11	−1	1	1	1	−1	1	1	−1	1	−1	54.43
6	12	1	1	1	−1	1	1	−1	1	−1	−1	87.91

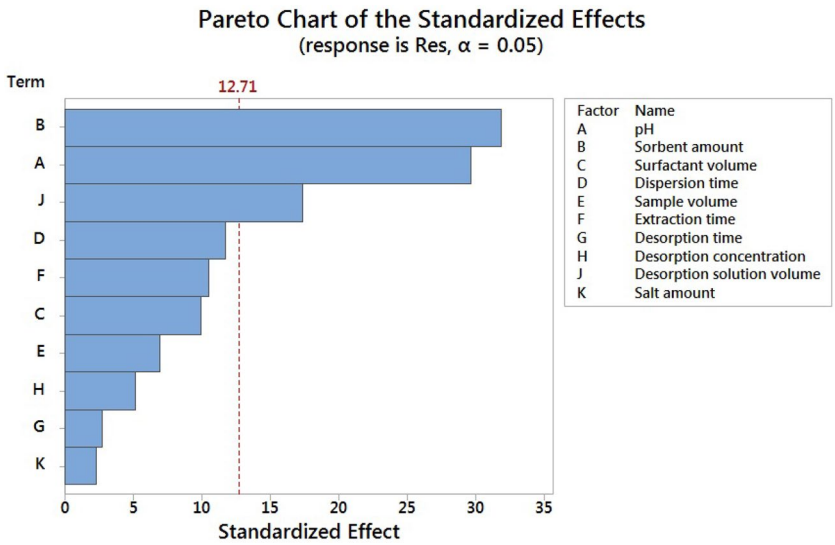

Fig. 4 Pareto chart obtained from analyzing the Plackett–Burman design

Central composite design

To optimize three factors, including pH, sorbent amount, and HNO_3 volume, selected as significant factors in the screening step, a central composite design (CCD) consisting of twenty experiments was created. The experimental runs were performed in random order to eliminate the effects of the uncontrolled variable. The selected factors and their levels are presented in ESM Table S3. Also, the CCD design and obtained responses are shown in Table 2. One-way analysis of variance (one-way ANOVA) was applied to investigate the factors and their interactions at 95% of the confidence limit (ESM Table S4). The p-value of the ANOVA table is a suitable parameter to determine the significant factors and interactions. A factor or interaction was known as a significant variable when its p-value is lesser than 0.05 at 95% of the confidence limit. According to ESM Table S4, all factors have a significant effect on the As(III) determination because their p-value is lower than 0.05, while all interactions between factors are not a significant variable for the As(III) determination. Also, the provided model by design is a significant variable, indicating the model was

Table 2 The central composite design matrix along with the obtained responses for the As (III) determination

Standard order	Run order	PtType	A	B	H	Response%
7	1	1	− 1.00000	1.00000	1.00000	31.82
20	2	0	0.00000	0.00000	0.00000	66.52
1	3	1	− 1.00000	− 1.00000	− 1.00000	37.32
10	4	− 1	1.68179	0.00000	0.00000	76.86
6	5	1	1.00000	− 1.00000	1.00000	39.40
8	6	1	1.00000	1.00000	1.00000	66.02
16	7	0	0.00000	0.00000	0.00000	82.52
14	8	− 1	0.00000	0.00000	1.68179	24.92
4	9	1	1.00000	1.00000	− 1.00000	96.54
11	10	− 1	0.00000	− 1.68179	0.00000	31.38
19	11	0	0.00000	0.00000	0.00000	83.76
9	12	− 1	− 1.68179	0.00000	0.00000	23.17
12	13	− 1	0.00000	1.68179	0.00000	74.65
3	14	1	− 1.00000	1.00000	− 1.00000	64.64
15	15	0	0.00000	0.00000	0.00000	62.52
17	16	0	0.00000	0.00000	0.00000	81.13
18	17	0	0.00000	0.00000	0.00000	80.89
13	18	− 1	0.00000	0.00000	− 1.68179	72.12
2	19	1	1.00000	− 1.00000	− 1.00000	73.22
5	20	1	− 1.00000	− 1.00000	1.00000	5.50

fitted well with responses. The p-value of lack of fit (0.985) is also higher than 0.05 and showed that this parameter is a nonsignificant variable that confirmed the suggested model was fitted well with responses. Central composite design can provide a quadratic equation to describe the relationship between factors and interactions with the As (III) extraction efficiency as follows:

$$\text{Response} = 76.13 + 16.56A + 12.91B - 8.66A * A - 7.60B * B - 9.19J * J - 0.46A * B + 0.04A * J + 0.29B * J \quad (1)$$

The obtained equation was fitted well with the responses because of the high R-squared (96.17%) and adjusted R-squared (92.73%). Besides, the equation can reasonably predict the response because the predicted R-squared of the equation is equal to 92.16% and more than 85. According to Eq. 1, the pH of the sample solution (A) is a critical factor with a positive effect on the As(III) determination due to its regression coefficient (16.56) in Eq. 1 is the highest, indicating that the As(III) extraction efficiency was increased with increasing the pH value. In other words, the appropriate electrostatic interactions between the sorbent surface and the As(III) ion were increased by increasing pH value, which leads to an increase in the As(III) extraction efficiency. The next factor with a negative effect on the As(III) extraction efficiency is the nitric acid volume (J) as a desorption solution. Obviously, the As(III) extraction efficiency was decreased with increasing the nitric acid volume due to dilution of As(III) ion concentration in the desorption solution. The sorbent amount (B) is the next significant factor with a positive effect on the As(III) extraction efficiency. It is because of the increase in the number of sites and functional groups on the sorbent surface with increasing the sorbent amount for interaction with the As(III) ions. All interactions between factors have no significant effects on the As(III) extraction efficiency based on their p-value, and so their regression coefficient is low in the obtained equation.

The optimization plot of the design for the As(III) determination is presented in Fig. 5. Based on this plot, the optimal values of significant factors, including pH, sorbent amount, and nitric acid volume, were determined to be 8.1, 30 mg, and 148 µL with the desirability of 0.986 and predicted extraction recovery of 95.3, respectively. The optimum values of all factors are summarized in ESM Table S5. The pH effect in the presence of CTAB in the extraction efficiency of As (III) species can be explained by the adsorption of CTAB on the sorbent surface. The pH_{zpc} of magnetic Fe_3O_4/chitosan is about 5.2, and so, the surface charge of the sorbent at the optimum pH (8.1) is negative [40]. CTAB was adsorbed on the sorbent through an electrostatic attraction to create a neutral surface on the sorbent to interact with H_3AsO_3 (pKa 9.2) as the dominant As (III) species in pH 8.1[41].

Investigating the effect of interference ions

Different species may be effective in measuring As(III) ions by the proposed method. Therefore, the effects of various species such as various cations and anions on the measurement of As(III) ions were evaluated. An ion interfered in the analyte determination when that ion causes a variation in the analyte absorbance of more than ± 5%[17]. For this purpose, a standard solution of As(III) ion (20.0 mL, 1.0 µg L^{-1}) was subjected to a 100-fold excess of a cation or anion as an interfering ion. The As(III) ion in the obtained solution was determined based on the proposed method under the optimum condition. The results are listed in Table 3, indicating that none of the studied ions had a significant effect on the measurement of As(III) ions. The variation in the absorbance of the As (III) solution created by most of the studied ions was less than ± 5%. Only two anions containing phosphate and silicate showed a significant interference in the As (III) measurement by the proposed method. Therefore, this method can be used to measure As(III) ions in different sample solutions without significant matrix effects for most ions in the solution.

Validation of the method and figures of merit

For the assessment of the proposed method, the analytical figures of merit were evaluated and determined. Under the optimized conditions, the calibration curve of the As(III)

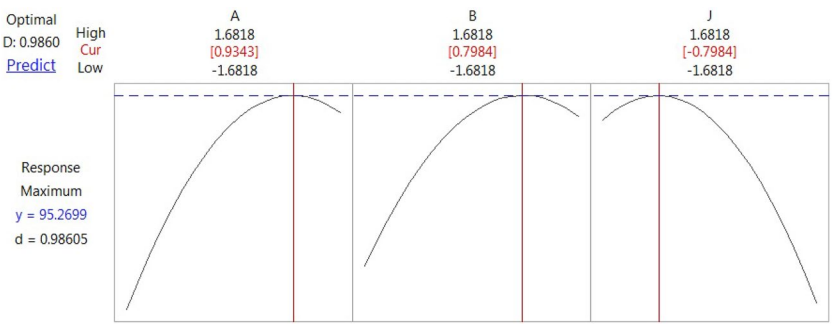

Fig. 5 Optimization plot of the central composite design for the As(III) determination

Table 3 Interference study for the determination of 1.0 μg L^{-1} of As (III) under the optimum conditions

Interfering ion	Concentration (μg L^{-1})	Variations of absorbance (%)
Co(II)	100	+4.26
Fe(II)	100	+1.85
As (V)	100	+4.79
Methyl arsenate	100	+4.13
Dimethyl arsenate	100	+3.89
Cu(II)	100	+2.05
Zn(II)	100	+2.05
Cr(III)	100	+3.71
Pt(II)	100	+3.04
Ag(I)	100	−1.92
Au(III)	100	+2.01
Mn(II)	100	+1.06
Hg(II)	100	+2.46
Ni(II)	100	−3.03
Pb(II)	100	+1.10
Ca(II)	200	+1.05
Mg(II)	200	+0.72
Na(I)	200	+1.04
K(I)	200	+0.94
I^-	100	+1.09
Cl^-	100	+1.21
SO_4^{-2}	100	+1.89
CH_3COO^-	100	+1.11
PO_4^{3-}	100	−7.64
SiO_3^{2-}	100	−8.23

determination was plotted using the standard solution of As(III) ion. The calibration curve for the As(III) determination was linear in the range of 0.009–10.0 μg L^{-1} with a determination coefficient of 0.9903. LOD and LOQ for target analytes were calculated using $3S_b/m$ and $10S_b/m$, where S_b and m were the standard deviation of the blank sample and calibration carve slope, respectively. LOD and LOQ for the As(III) ion determination were 0.003 and 0.009 μg L^{-1}, respectively. RSD for five times of the As(III) determination (0.1 μg L^{-1}) under the optimum conditions was 3.27%. Enrichment factor (EF) was obtained based on the ratio of the calibration curve slope of the sample after the microextraction of the sample to the slope of the calibration curve before the microextraction of the sample solution and was equal to 21.84. The method accuracy was investigated using a certified reference material (TraceCERT®, 75,016) with diluting in distilled water to a concentration of 0.5 μg L^{-1}. The experiments were repeated three times under the same conditions. The As(III) concentration in CRM was founded to be 0.97 ± 0.03 μg L^{-1} that showed a good agreement with the certified amount of 1 μg L^{-1}.

Table 4 The results of method accuracy in the real samples ($n = 3$)

Sample	Added (μg L^{-1})	Founded (μg L^{-1})	%RR	%RSD
Tap water	0.00	0.017	–	3.41
	0.05	0.065	96.0	3.29
	0.50	0.503	97.2	3.17
River water	0.00	0.028	–	3.64
	0.05	0.076	96.0	3.50
	0.50	0.515	97.4	3.31
Urine	0.00	ND[1]		–
	0.05	0.048	96.0	3.79
	0.50	0.487	97.4	3.61
Apple juice	0.00	0.023	–	4.12
	0.05	0.070	94.0	3.94
	0.5	0.507	96.8	3.95
Grape juice	0.00	0.014	–	4.54
	0.05	0.061	94.0	4.27
	0.5	0.496	96.4	3.98

[1]Not detect; LOD = 0.003 μg L^{-1}

Real sample analysis

To evaluate the applicability of the proposed method for the As(III) ion determination in real samples, several real samples, including water, urine, and fruit juice samples, were investigated using the proposed method. Water samples were obtained from the outskirts of Mashhad (Iran). Urine samples were obtained from a 35 year-old man. Before sampling, the reason for sampling was explained to the volunteer, and the sampling was done with his consent. Fruit juice samples (grapes and apples) prepared by Alifard company (Saveh, Iran) were purchased from a local supermarket in Mashhad (Iran). All urine, fruit juice, and water samples were filtered for separating impurities and spiked with the As (III) standard solution at two concentrations of 0.05 and 0.5 μg L^{-1}. The proposed procedure was applied successfully for studying the method's accuracy and evaluating the matrix effects of the real samples. The results are presented in Table 4, indicating that the relative recovery of the As(III) ions is in the range of 94.0–97.4% with a relative standard deviation of 3.17–4.54% (Table 4). The obtained results showed the method is suitable for the As(III) determination with non-significant matrix effects under the studied concentration of interfering ions.

The sorbent reusability

Sorbent reuse for As(III) ion extraction was studied as an essential parameter. For this purpose, the sorbent after the As(III) ion desorption with nitric acid was washed with distilled water and then used to re-extract the As(III) ion in the sample solution under the optimum conditions. The

extraction efficiencies of As(III) ions were 97.2, 94.4, 89.6, and 76.3 for the four extraction–desorption cycles, respectively. These results indicate that the sorbent can be used for up to three extraction–desorption cycles of As(III) ions.

Comparison with other methods

Several methods were selected and compared with the proposed method for As(III) ion determination (Table 5). The magnetic Fe_3O_4@chitosan mesopores as a DμSPE sorbent was displayed a good capability to pre-concentrate and extract the As (III) ion. Also, a combination of the DμSPE procedure with the hydride generation method shows a low detection limit in comparison with other methods. Besides, the proposed method was reported a lower LOD and wider linearity from the previous procedure. Another advantage of the technique is a simple combination of the microextraction method with the ETAAS technique. The commercial availability of magnetic Fe_3O_4 and the simple chemical preparation method for the sorbent preparation through the modification of magnetic Fe_3O_4 with chitosan as a green and efficient sorbent encourages the excellent application of the procedure for the As(III) ion determination.

Conclusion

In this research, a combination of surfactant-assisted magnetic dispersive micro-solid-phase extraction as a sample preparation method with hydride generation procedure was developed to measure As(III) species in various real samples. In the sample preparation procedure, a surfactant as a dispersion agent was employed to decrease the ultrasonic time and the possibility of sorbent degradation. Besides, the surfactant can increase the sorbent dispersion efficiency and lead to an increase in the analyte extraction efficiency through a reduction in the sorbent size and an increase in the sorbent surface area. For this purpose, the effects of three surfactants including sodium dodecyl sulfate, hexadecyltrimethylammonium bromide, and triton X100 were evaluated as a dispersion agent on the As(III) extraction, indicating that hexadecyltrimethylammonium has the highest significant effect on the As(III) determination due to increase in the sorbent dispersion efficiency. Magnetic Fe_3O_4/chitosan was synthesized as a magnetic and green sorbent with a simple chemical method and characterized using FTIR spectrum, SEM, and TEM images. The proposed microextraction procedure for the As(III) determination with a low sorbent and sample solution consumption, suitable extraction time, and use of green sorbent follows the principles of green chemistry. The study of the effects of interfering ions showed that the cations and anions under investigation do not interfere

Table 5 Comparison of different methods for the As(III) determination

Matrix	Technique/sorbent	Instrument	LDR	LOD	Reference
-	SPME/functionalized nanoparticles of Al_2O_3	Graphite furnace AAS	As(III): 5.0×10^3–2.8×10^5 μg/L As (total): 8.0×10^3–2.6×10^5 μg/L	As(III): 1.81×10^3 μg/L As(total): 1.97×10^3 μg/L	[42]
Water samples	HF-SPME/ TiO_2 nanoparticle and composite	Atomic florescence spectroscopy	As(III): 0.01–3.00 μg/L	0.003 μg/L	[43]
Rice	SPME	HG-AAS	0.03–0.6 mg/Kg	0.02 mg/Kg	[44]
Water samples	SPE/AlOH gel	HG-AFS	0.05–10 μg/L	0.003 μg/L	[45]
Garlic	D-μ-SPE/MWCNT	ET-AAS		0.007 μg/L	[46]
Water and urine samples	USA-DSL-MPME/NH2-UVM,nano-SiO_2	ET-AAS	Natural water:0.02–1.65 μg/L Urine samples: 0.02–1.69 μg/L	Natural water: 0.0033 μg/L Urine: 0.0027 μg/L	[47]
Natural water	USAE-SFODME	ET-AAS	0.05–2.0 μg/L		[48]
Water samples	Amberlit SPE	ET-AAS	0.42–40 μg/L	0.126 μg/L	[49]
Natural water	SPME/AAPTS-MWCNT	ICP-MS	0.05–1.00 μg/L	0.015 μg/L	[50]
environmental water	SPME/Fe_3O_4-SiO_2-NH_2	ICP-MS	–	2.1×10^{-4} μg/L	[51]
Water samples	SPE/Fe_3O_4-Mg–Al	Chemiluminescence	5.0×10^3–5.0×10^6 μg/L	2.0×10^3 μg/L	[52]
Water samples	DμSPE/magnetic Fe_3O_4/chitosan	HG-ET-AAS	0.009–10.0 μg/L	0.002 μg/L	This work

significantly with the As(III) measurement. Comparison of the proposed method with other methods indicated that the method has outstanding sensitivity with a wider linear range and lower detection limit than most of the previous methods. The most important advantages of the method include simplicity, low consumption of organic solvents and sample solution, good enrichment factor, use of green sorbent, and high sensitivity without the need for sophisticated devices for determining As(III) species. Besides, the method was successfully utilized to analyze river water, tap water, urine, apple juice, and grape juice samples with proper relative recovery in 94.0–97.4% and relative standard deviation in the range of 3.17–4.54%.

Supplementary Information The online version contains supplementary material available at https://doi.org/10.1007/s13738-021-02457-9.

Acknowledgements The authors thank of Islamic Azad University branch of Mashhad for the financial support of this work.

References

1. M. Arjomandi, H. Shirkhanloo, A review: analytical methods for heavy metals determination in environment and human samples. Anal. Methods Environ. Chem. J. **2**(03), 97–126 (2019)
2. I. Ali, Microwave assisted economic synthesis of multi walled carbon nanotubes for arsenic species removal in water: batch and column operations. J. Mol. Liq. **271**, 677–685 (2018)
3. D.T. Heitkemper, N.P. Vela, K.R. Stewart, C.S. Westphal, Determination of total and speciated arsenic in rice by ion chromatography and inductively coupled plasma mass spectrometry. J. Anal. At. Spectrom. **16**(4), 299–306 (2001)
4. I. Ali, Z.A. Al-Othman, A. Alwarthan, M. Asim, T.A. Khan, Removal of arsenic species from water by batch and column operations on bagasse fly ash. Environ. Sci. Pollut. Res. **21**(5), 3218–3229 (2014)
5. I. Ali, C.K. Jain, Advances in arsenic speciation techniques. Int. J. Environ. Anal. Chem. **84**(12), 947–964 (2004)
6. M. Hemmati, M. Rajabi, A. Asghari, Magnetic nanoparticle based solid-phase extraction of heavy metal ions: a review on recent advances. Microchim. Acta **185**(3), 160 (2018)
7. S.-H. Chen, Y.-X. Li, P.-H. Li, X.-Y. Xiao, M. Jiang, S.-S. Li, W.-Y. Zhou, M. Yang, X.-J. Huang, W.-Q. Liu, Electrochemical spectral methods for trace detection of heavy metals: a review. TrAC, Trends Anal. Chem. **106**, 139–150 (2018)
8. I. Ali, M. Suhail, O.M. Alharbi, I. Hussain, Advances in sample preparation in chromatography for organic environmental pollutants analyses. J. Liq. Chromatogr. Relat. Technol. **42**(5–6), 137–160 (2019)
9. I. Ali, V.K. Gupta, H.Y. Aboul-Enein, A. Hussain, Hyphenation in sample preparation: advancement from the micro to the nano world. J. Sep. Sci. **31**(11), 2040–2053 (2008)
10. M. Ghorbani, P. Mohammadi, M. Keshavarzi, M.H. Saghi, M. Mohammadi, A. Shams, M. Aghamohammadhasan, Simultaneous determination of organophosphorus pesticides residues in vegetable, fruit juice, and milk samples with magnetic dispersive micro solid-phase extraction and chromatographic method; Recruitment of simplex lattice mixture design for optimization of novel sorbent composites. Analytica Chimica Acta **1178**, 338802 (2021)
11. M. Ghorbani, T. Pedramrad, M. Aghamohammadhasan, O. Seyedin, H. Akhlaghi, N.A. Lahoori, Simultaneous clean-up and determination of Cu (II), Pb (II) and Cr (III) in real water and food samples using a magnetic dispersive solid phase microextraction and differential pulse voltammetry with a green and novel modified glassy carbon electrode. Microchem. J. **147**, 545–554 (2019)
12. M. Aghamohammadhasan, V. Ghashamsham, M. Ghorbani, M. Chamsaz, M. Masrournia, T. Pedramrad, H. Akhlaghi, Preconcentration of gadolinium ion by solidification of floating organic drop microextraction and its determination by UV-Vis spectrophotometry. Eurasian J. Anal. Chem. **12**(8), 1621–1629 (2017)
13. M. Ghorbani, S. Akbarzade, M. Aghamohammadhasan, O. Seyedin, N.A. Lahoori, Pre-concentration and determination of cadmium and lead ions in real water, soil and food samples using a simple and sensitive green solvent-based ultrasonic assisted dispersive liquid–liquid microextraction and graphite furnace atomic absorption spectrometry. Anal. Methods **10**(17), 2041–2047 (2018)
14. A. Chisvert, S. Cárdenas, R. Lucena, Dispersive micro-solid phase extraction. TrAC Trends Anal. Chem. **112**, 226–233 (2019)
15. P. Mohammadi, M. Ghorbani, P. Mohammadi, M. Keshavarzi, A. Rastegar, M. Aghamohammadhassan, A. Saghafi, Dispersive micro solid-phase extraction with gas chromatography for determination of Diazinon and Ethion residues in biological, vegetables and cereal grain samples, employing D-optimal mixture design. Microchem. J. **160**, 105680 (2021)
16. M. Ghorbani, M. Aghamohammadhassan, H. Ghorbani, A. Zabihi, Trends in sorbent development for dispersive micro-solid phase extraction. Microchem. J. **158**, 105250 (2020)
17. E. Hosseini, M. Chamsaz, M. Ghorbani, A novel ultrasonic assisted dispersive solid phase microextraction for preconcentration of beryllium ion in real samples using CeO_2 nanoparticles and its determination by flame atomic absorption spectrometry. Eurasian J. Anal. Chem. **13**(1), 1–10 (2017)
18. Z. Moradi, E.A. Dil, A. Asfaram, Dispersive micro-solid phase extraction based on Fe_3O_4@ SiO_2@ TI-MOF as a magnetic nanocomposite sorbent for the trace analysis of caffeic acid in the medical extracts of plants and water samples prior to HPLC-UV analysis. Analyst **144**(14), 4351–4361 (2019)
19. I. Ali, Nano-hyphenation technologies, Laboratory plus international (2009) pp 14–16.
20. T. Boontongto, K. Siriwong, R. Burakham, Amine-functionalized metal-organic framework as a new sorbent for vortex-assisted dispersive micro-solid phase extraction of phenol residues in water samples prior to HPLC analysis: experimental and computational studies. Chromatographia **81**(5), 735–747 (2018)
21. L. Adlnasab, M. Ezoddin, R.A. Shojaei, F. Aryanasab, Ultrasonic-assisted dispersive micro solid-phase extraction based on melamine-phytate supermolecular aggregate as a novel bio-inspired magnetic sorbent for preconcentration of anticancer drugs in biological samples prior to HPLC-UV analysis. J. Chromatogr. B **1095**, 226–234 (2018)
22. M. Ghorbani, M. Aghamohammadhassan, M. Chamsaz, H. Akhlaghi, T. Pedramrad, Dispersive solid phase microextraction. TrAC, Trends Anal. Chem. **118**, 793–809 (2019)
23. F. Priego-Capote, L. de Castro, Ultrasound-assisted digestion: A useful alternative in sample preparation. J. Biochem. Biophys. Methods **70**(2), 299–310 (2007)
24. D.S. Júnior, F.J. Krug, M.G. de Pereira, M. Korn, Currents on ultrasound-assisted extraction for sample preparation and spectroscopic analytes determination. Appl. Spectr. Rev. **41**(3), 305–321 (2006)
25. M. Ghorbani, M. Esmaelnia, M. Aghamohammadhasan, H. Akhlaghi, O. Seyedin, Z.A. Azari, Preconcentration and determination of fluoxetine and norfluoxetine in biological and water samples with β-cyclodextrin multi-walled carbon nanotubes as

a suitable hollow fiber solid phase microextraction sorbent and high performance liquid chromatography. J. Anal. Chem. **74**(6), 540–549 (2019)
26. M. Ghorbani, M. Chamsaz, G.H. Rounaghi, Ultrasound-assisted magnetic dispersive solid-phase microextraction: a novel approach for the rapid and efficient microextraction of naproxen and ibuprofen employing experimental design by high-performance liquid chromatography. J. Sep. Sci. **39**(6), 1082–1089 (2016)
27. P. Hu, X. Wang, Z. Wang, R. Dai, W. Deng, H. Yu, K. Huang, Recent developments of hydride generation in non-atomic spectrometric methods. TrAC Trends Anal. Chem. **119**, 115617 (2019)
28. P. Liang, L. Peng, P. Yan, Speciation of As (III) and As (V) in water samples by dispersive liquid-liquid microextraction separation and determination by graphite furnace atomic absorption spectrometry. Microchim. Acta **166**(1–2), 47–52 (2009)
29. M. Segura, J. Muñoz, Y. Madrid, C. Cámara, Stability study of As (III), As (V), MMA and DMA by anion exchange chromatography and HG-AFS in wastewater samples. Anal. Bioanal. Chem. **374**(3), 513–519 (2002)
30. D. Wallschläger, N.S. Bloom, Determination of selenite, selenate and selenocyanate in waters by ion chromatography-hydride generation-atomic fluorescence spectrometry (IC-HG-AFS). J. Anal. At. Spectrom. **16**(11), 1322–1328 (2001)
31. M.A. Suner, V. Devesa, O. Muñoz, D. Vélez, R. Montoro, Application of column switching in high-performance liquid chromatography with on-line thermo-oxidation and detection by HG-AAS and HG-AFS for the analysis of organoarsenical species in seafood samples. J. Anal. At. Spectrom. **16**(4), 390–397 (2001)
32. I. De Gregori, W. Quiroz, H. Pinochet, F. Pannier, M. Potin-Gautier, Simultaneous speciation analysis of Sb (III), Sb (V) and $(CH_3)_3SbCl_2$ by high performance liquid chromatography-hydride generation-atomic fluorescence spectrometry detection (HPLC-HG-AFS): application to antimony speciation in sea water. J. Chromatogr. A **1091**(1), 94–101 (2005)
33. L.V. Candioti, M.M. De Zan, M.S. Camara, H.C. Goicoechea, Experimental design and multiple response optimization. Using the desirability function in analytical methods development. Talanta **124**, 123–138 (2014). https://doi.org/10.1016/j.talanta.2014.01.034
34. S.A. Weissman, N.G. Anderson, design of experiments (DoE) and process optimization. A review of recent publications. Org. Process Res. Dev. **19**(11), 1605–1633 (2015)
35. K. Sharif, M. Rahman, J. Azmir, A. Mohamed, M. Jahurul, F. Sahena, I. Zaidul, Experimental design of supercritical fluid extraction–A review. J. Food Eng. **124**, 105–116 (2014)
36. M. Seyedsadjadi, S. Babaei, N. Farhadyar, Preparation of surface modified magnetic iron oxide nanoparticles and study of their colloidal behavior. Int. J. Nano Dimens. **5**(3), 279 (2014)
37. A. Kaushik, R. Khan, P.R. Solanki, P. Pandey, J. Alam, S. Ahmad, B. Malhotra, Iron oxide nanoparticles–chitosan composite based glucose biosensor. Biosens. Bioelectron. **24**, 676–683 (2008). https://doi.org/10.1016/j.bios.2008.06.032
38. E.M. Becker, M.B. Dessuy, W. Boschetti, M.G.R. Vale, S.L. Ferreira, B. Welz, Development of an analytical method for the determination of arsenic in gasoline samples by hydride generation–graphite furnace atomic absorption spectrometry. Spectrochim. Acta, Part B **71**, 102–106 (2012)
39. Z. Chen, G. Yu, Q. Wang, Effects of climate and forest age on the ecosystem carbon exchange of afforestation. J. For. Res. **31**(2), 365–374 (2020)
40. N. Subedi, A. Lähde, E. Abu-Danso, J. Iqbal, A. Bhatnagar, A comparative study of magnetic chitosan (Chi@ Fe_3O_4) and graphene oxide modified magnetic chitosan (Chi@ Fe_3O_4GO) nanocomposites for efficient removal of Cr (VI) from water. Int. J. Biol. Macromol. **137**, 948–959 (2019)
41. S.D. Wilson, W.R. Kelly, T.R. Holm, J.L. Talbott, Arsenic removal in water treatment facilities: survey of geochemical factors and pilot plant experiments, Illinois State Water Survey, 2004.
42. S. Hassanpoor, G. Khayatian, A.R.J. Azar, Ultra-trace determination of arsenic species in environmental waters, food and biological samples using a modified aluminum oxide nanoparticle sorbent and AAS detection after multivariate optimization. Microchim. Acta **182**(11–12), 1957–1965 (2015)
43. Z. Es'haghi, S. Taghizade, A. Mazloomi-Bajestani, Arsenic removal from water/wastewater using nanoparticle-assisted hollow fiber solid-phase microextraction combined with hydride generation–atomic fluorescence spectroscopy. J. Iran. Chem. Soc. **11**(5), 1421–1428 (2014)
44. R.R. Rasmussen, Y. Qian, J.J. Sloth, SPE HG-AAS method for the determination of inorganic arsenic in rice—results from method validation studies and a survey on rice products. Anal. Bioanal. Chem. **405**(24), 7851–7857 (2013)
45. F. Deng, R. Dong, K. Yu, X. Luo, X. Tu, S. Luo, L. Yang, Determination of trace total inorganic arsenic by hydride generation atomic fluorescence spectrometry after solid phase extraction-preconcentration on aluminium hydroxide gel. Microchim. Acta **180**(5–6), 509–515 (2013)
46. A.C. Grijalba, L.B. Escudero, R.G. Wuilloud, Ionic liquid-assisted multiwalled carbon nanotube-dispersive micro-solid phase extraction for sensitive determination of inorganic As species in garlic samples by electrothermal atomic absorption spectrometry. Spectrochim. Acta, Part B **110**, 118–123 (2015)
47. H. Shirkhanloo, M. Ghazaghi, A. Rashidi, A. Vahid, Arsenic speciation based on amine-functionalized bimodal mesoporous silica nanoparticles by ultrasound assisted-dispersive solid-liquid multiple phase microextraction. Microchem. J. **130**, 137–146 (2017)
48. M. Asadollahzadeh, N. Niksirat, H. Tavakoli, A. Hemmati, P. Rahdari, M. Mohammadi, R. Fazaeli, Application of multi-factorial experimental design to successfully model and optimize inorganic arsenic speciation in environmental water samples by ultrasound assisted emulsification of solidified floating organic drop microextraction. Anal. Methods **6**(9), 2973–2981 (2014)
49. A. Tunçeli, G. Ocak, O. Acar, A.R. Türker, Development of a method for speciation of inorganic arsenic in waters using solid phase extraction and electrothermal atomic absorption spectrometry. Int. J. Environ. Anal. Chem. **95**(14), 1395–1411 (2015)
50. H. Peng, N. Zhang, M. He, B. Chen, B. Hu, Simultaneous speciation analysis of inorganic arsenic, chromium and selenium in environmental waters by 3-(2-aminoethylamino) propyltrimethoxysilane modified multi-wall carbon nanotubes packed microcolumn solid phase extraction and ICP-MS. Talanta **131**, 266–272 (2015)
51. C. Huang, W. Xie, X. Li, J. Zhang, Speciation of inorganic arsenic in environmental waters using magnetic solid phase extraction and preconcentration followed by ICP-MS. Microchim. Acta **173**(1–2), 165–172 (2011)
52. H. Abdolmohammad-Zadeh, Z. Talleb, Speciation of As (III)/As (V) in water samples by a magnetic solid phase extraction based on Fe_3O_4/Mg–Al layered double hydroxide nano-hybrid followed by chemiluminescence detection. Talanta **128**, 147–155 (2014)